Early intrinsic plasticity of ACC engram neurons defines memory formation and precision

Authors: Senka Hadzibegovic[1,2]†, Liangying Zhu[1,2]†, Melanie Ginger[1,2], Rafael De Sa[1,2], Katy le Corf[1,2], Maria Gueidão Costa[1,2,5], Olivier Nicole[2,3], Bruno Bontempi[2,4]‡*, Andreas Frick[1,2]‡*

Affiliations:

[1]INSERM, U1215 Neurocentre Magendie, Bordeaux, 33077, France.

[2]University of Bordeaux, Bordeaux, 33077, France.

[3]CNRS, IINS, UMR 5297, Bordeaux, 33077, France.

[4]CNRS, INCIA, UMR 5287, Bordeaux, 33077, France.

[5]University of the Basque Country, Leioa 48940, Spain

*Corresponding authors. Email: bruno.bontempi@u-bordeaux.fr, andreas.frick@inserm.fr

†These authors contributed equally to this work

‡ These authors contributed equally to this work or co-last senior authors

Abstract:

Learning induces an early tag of prefrontal cortex neurons implicated in long-term memory storage, but this tag's nature, functional role, and time course are unknown. Using a c-fos dependent genetic and viral system for the labeling and manipulation of putative engram neurons of the anterior cingulate cortex (ACC) together with behavior and in vitro electrophysiology, we found that contextual fear learning triggered an increase in the neuron-wide intrinsic excitability specifically of ACC engram neurons. This plasticity was expressed over several days during the early memory phase and required for enduring memory storage. Pharmacogenetic manipulation of the engram neurons' intrinsic excitability during its plastic phase altered the strength and context-precision of enduring fear memories. Moreover, this manipulation prevented the memory decline usually caused by an interference event. In contrast, excitability manipulation or interference during remote memory phases did not influence long-term memory retrieval; their impact is thus strongly correlating with the time course of intrinsic plasticity. These findings shed light on the functional role of intrinsic plasticity of ACC engram neurons in long-term memory storage. Associative learning strongly engages ACC engram neurons and triggers neuron-wide intrinsic plasticity. This plasticity is transiently expressed and necessary for the consolidation and specificity of long-term memory.

INTRODUCTION

Associative memories are gradually embedded within neocortical circuits during systems-level memory consolidation, the process by which remote memories acquire stability and persistence over time (de Sousa et al., 2019; Frankland and Bontempi, 2005). Early (during learning) tagging of the same cortical circuits that will later act as the permanent repository of memory engrams has been identified as a prerequisite for successful consolidation (Bero et al., 2014; Kitamura, 2017; Lesburguères et al., 2011; Roy et al., 2022). Thus, cortical memory engrams are thought to undergo a time-dependent maturation process from an initially immature (dormant, non-accessible) to an active (retrievable) state (Frankland et al., 2004; Tayler et al., 2013). However, the specific processes regulating engram transformation and enduring storage remain elusive.

The allocation of neurons to a given memory engram does not occur randomly. Instead, highly excitable neurons within a connected ensemble are preferentially earmarked for integration into that engram (Cai et al., 2016; Rashid et al., 2016). In corollary, changes in neuronal intrinsic excitability could provide a key regulatory determinant for the integration of engram neurons. In addition, neuron-wide intrinsic excitability plasticity (IEP) has been described in several brain regions following learning paradigms (Frick and Johnston, 2005; Titley et al., 2020; Zhang and Linden, 2003). However, while changes in the synaptic strength and connectivity map and of engram ensembles are widely viewed mechanisms for the establishment of enduring memories, the role of IEP in this process is unknown. Neuron-wide IEP would tune the responsiveness of that neuron to its synaptic inputs and prime it to undergo further plasticity (i.e., metaplasticity; (Abraham and Bear, 1996)) such as synaptic strength and connectivity changes. As a result, this mechanism may dictate the fate of engram neurons during systems memory consolidation and play a permissive role in the establishment of enduring memories. To fulfill this role, we hypothesized that associative learning tasks activate anterior cingulate cortex (ACC) engram ensembles and trigger neuron-wide IEP in these neurons as part of the early mechanisms of the memory trace. These changes occur as a consequence of early activation of these neurons (1), are transient (early-phase memory consolidation) (2), and are both permissive and necessary for the network to store memories more permanently in remote memory (3).

RESULTS

Anterior cingulate cortex (ACC) engram neurons are strongly engaged during learning

The prevailing literature suggests a role for the ACC in remote but not early phases of memory formation (Dixsaut and Gräff, 2021; Frankland et al., 2004). To explore whether these ACC engram ensembles are tagged by the learning experience (nascent engram neurons) and their functional role in later memory expression, we employed a *c-fos*-dependent labeling approach that combines double-transgenic "tet-tag" mice with virus-mediated expression of a fluorescent marker (mCherry) during contextual fear conditioning (CFC) (Fig. 1A). CFC induces a lasting fear memory of a single event, enabling rigorous temporal control of neuronal tagging. In the presence of doxycycline (dox), no labeling was observed following CFC (Fig. 1B). Conversely, CFC performed during a defined dox-off time window led to the expression of the fluorescence marker in engaged ACC neurons (Fig. 1B).

Robust CFC-induced fluorescence marker expression was present one day following the learning experience and persisted for at least 30 days, demonstrating early and stable labeling of putative ACC engram neurons (Fig. 1D). The number of tagged ACC neurons was significantly greater in the CFC condition compared with those where mice were placed in the conditioning environment without the aversive reinforcement of the foot shocks (context-only, CTX) or kept in the home-cage (HC) (Fig. 1C, 1D). Early-phase memory retrieval of the CFC group did not reactivate these original putative ACC engram neurons when compared to the CTX and HC groups (ratio mCherry+/GFP+ neurons; Fig. 1E). Conversely, these neurons were strongly reactivated during remote memory retrieval (Fig. 1E), correlating with the formation of a robust fear memory (Fig. 1F & 1G).

These findings demonstrate that learning tags nascent ACC engram ensembles that are strongly implicated in the expression of remote fear memory. Conversely, these ensembles are not reactivated during the early phases of memory retrieval; rather they remain in a silent state.

Associative learning triggers neuron-wide IEP in ACC engram neurons

Our data show that putative fear-memory-related ACC engram neurons are tagged already during the learning phase. To examine whether these neurons undergo plastic changes in their intrinsic excitability triggered by the learning event, we evaluated their intrinsic properties during the early-phase memory consolidation, one to three days post-CFC. We performed whole-cell recordings of labeled neurons (CFC-YFP+ neurons, Fig 2A) within acute ACC brain slices (Fig. 2B), focusing on thick-tufted layer 5 (L5) pyramidal tract (PT) neurons (Fig. 2C), which represent a major type

of neocortical output neurons. We probed the plasticity of their intrinsic properties by comparing them to those of labeled neurons from the CTX group (CTX-YFP+ neurons) to define changes specific to the learning experience and not caused by background activity or an unrelated experience.

We discovered that CFC induced a significant increase in the neuron-wide intrinsic excitability of putative ACC engram neurons compared to control neurons (Fig. 2D-N; for a complete list of measures see Supplementary Table 1). This increased excitability was expressed as a greater number of action potentials (APs) triggered by injected current (Fig. 2D). In addition, individual APs were elicited at a more hyper-polarized threshold (Fig. 2E), displayed a greater amplitude (Fig. 2F), were broader (increased half-width; Fig. 2G), and exhibited a reduced upstroke velocity (max dv/dt; Fig. 2H). In agreement with the hyper-polarized shift in the AP threshold, the minimum current to induce an AP (rheobase) was reduced (Fig. 2I) despite a more hyper-polarized resting membrane potential (RMP) (Fig. 2J). Furthermore, the amplitude of the medium after-hyperpolarization (mAHP) following a train of APs was reduced for the highest AP frequencies tested (Fig. 2K). However, this reduced mAHP amplitude had no obvious impact on the AP adaptation during a train of APs (Fig. 2L). Finally, we also found that the membrane time constant (tau) was prolonged, widening the temporal window for the integration of synaptic inputs (Fig. 2M).

Our results show that contextual fear conditioning modifies several excitability features of the L5-PT subnetwork of putative ACC engram neurons in a learning-specific manner, leading to a plastic increase in their neuron-wide intrinsic excitability. Notably, this plasticity is evident one day post-CFC and persists for at least three days.

Neuron-wide IEP is expressed during early- but not remote-phase memory consolidation

We hypothesized that IEP would be transiently expressed during early-phase memory consolidation but not during the remote phase when memories have been mostly consolidated (>14 days post-CFC) since it would severely limit the neurons' storage capacity (Frick and Johnston, 2005). To test this, we assessed the intrinsic properties of CFC-labeled L5-PT neurons at 15-17 days post-CFC (Fig. 3A).

These measures confirmed our prediction, showing that the neuron-wide IEP has returned to naïve pre-learning values at remote memory phases. At 15–17 days post-CFC, the intrinsic excitability features were similar between putative engram ensembles (CFC-YFP+) and control neurons (CTX-YFP+) of the ACC (Suppl. Fig 1, Supplementary Table 2). Accordingly, the following intrinsic excitability measures of putative engram ensembles (CFC-YFP+) differed significantly between early- and remote-phase memory consolidation (values are normalized to those of CTX during early and remote phases, respectively; Fig 3B-I): AP number triggered by current injection (greater during early-phase; Fig 3B), AP peak amplitude (increased; Fig 3C), AP half-width (increased; Fig 3D), rheobase (reduced; Fig 3E), RMP (more depolarized; Fig 3F), mAHP amplitude (reduced; Fig 3G), ISI adaptation (reduced; Fig 3H), and tau (increased; Fig 3I). Conversely, there was no significant difference in the AP upstroke velocity (max dV/dt (Suppl. Fig 2), and only a trend for the AP threshold (more hyperpolarized during the early phase).

Our data shows that the learning-induced neuron-wide IEP of putative ACC engram neurons is expressed during the early but not the remote phase of memory consolidation.

Early IEP is necessary for the formation of remote fear memory

According to our hypothesis, neuron-wide IEP triggered by learning and expressed over several days alters the responsiveness of the engram ensemble and permits more enduring plastic changes which require repeated activation and more time to develop (Frick and Johnston, 2005). We therefore predicted that modulating the intrinsic excitability of ACC engram ensembles during its CFC-induced plastic phase would interfere with this functional role and either enhance or weaken the formation of enduring fear memories. We probed this by altering the intrinsic excitability of putative ACC engram neurons during different memory phases using a pharmacogenetic approach. Employing our tet-tagging systems, we expressed either an inhibitory (i) or excitatory (e) form of DREADD in these neurons following CFC (Fig. 4A). We then modulated the intrinsic excitability of these engram neurons for 7 consecutive days following CFC by administering CNO twice a day, and tested the consequence of this manipulation for remote fear memory expression (30 days post-CFC; Fig. 4A). We found that CNO stimulation of iDREADD-expressing ACC engram ensembles (including the L5-PT subnetwork) during the early-memory phase enhanced remote fear memory expression (manifested as increased freezing) in these mice (iDREADD/CNO group) when compared to control (i/eDREADD/saline group; Fig. 4B). In contrast, activating eDREADD

in tagged ACC engram ensembles reduced remote memory strength (eDREADD/CNO group; Fig. 4B).

These data show that pharmacogenetic interference with the intrinsic excitability state of ACC engram neurons during the early phase of memory consolidation can enhance or prevent enduring fear memory formation.

The context-specificity of remote fear memory is malleable during the intrinsic plasticity phase

In addition to the strength of fear expression, we wondered whether modulating the intrinsic excitability of ACC engram ensembles during early-phase memory consolidation could also improve the precision of the remote fear memory for the specific context. We assessed memory specificity by performing remote retrieval either in the original context (Context A) or in a new context (Context B) (Fig. 4A). Mice were divided into separate groups for retrieval in either Context A or B because we found that successive retrieval in both contexts attenuated fear expression in the second context (Supplementary Fig. 3). These experiments showed that the iDREADD/CNO group discriminated better between the two contexts, displaying an improved Context A-specific fear memory (Fig. 4B & C). Enhanced memory precision was reflected in both an increase in freezing in Context A and a decrease in freezing in Context B (Fig. 4C). In contrast, activating eDREADD in tagged ACC engram neurons resulted in an impaired contextual fear memory precision, eliminating the capacity to discriminate between a familiar context and an unfamiliar one (Fig. 4B & C). The differences in memory precision and strength between the three groups could not be explained by the original freezing score during CFC (Suppl. Fig. 4A&B), nor by the number of engram neurons that expressed DREADD (Supplementary Fig. 4C).

ACC engram ensembles were strongly reactivated by remote memory retrieval (Fig. 1E), and we wondered whether the increased memory strength/precision induced by iDREADD activation (Fig. 4B, C) would be reflected in an even greater reactivation of these neurons. Indeed, the reactivation ratio (% mCherry+/GFP+ neurons) following iDREADD-activation of ACC engram ensembles was significantly greater compared to the saline or eDREADD condition (Fig. 4D). In contrast, the number of retrieval-activated neurons itself was not altered (Supplementary Fig. 4D).

Our results show that changes in the neuron-wide state of the intrinsic excitability of ACC engram ensembles during early memory consolidation are essential for the enduring storage and precision

of fear memories; any modulation of the excitability state during its plastic phase crucially influences these features, correlating with the reactivation of the nascent ACC engram ensemble following its maturation.

Modulating the intrinsic excitability of ACC engram neurons during remote memory phases does not affect memory expression

We then investigated whether the efficacy of manipulating the intrinsic excitability of ACC engram neurons for improving memory performance was temporally limited, following a similar time course to that required for neuron-wide IEP. We manipulated the excitability of DREADD-expressing ACC engram neurons during remote-phase memory consolidation (CNO application 15–22 days following CFC) when the IEP had returned to naïve pre-learning levels (Fig. 3). Consistent with the temporal course of IEP, we observed no functional consequence on memory performance or context precision by either iDREADD or eDREADD activation during this remote memory time window (Fig. 4F & G, Supplementary Fig. 5). Similarly, in line with the correlation of memory strength and ACC engram ensemble reactivation during remote memory phases, this ratio was also not affected by excitability modulation at this remote phase (Fig. 4H).

Our data shows that the IEP of ACC engram ensembles and the functional consequence of manipulating their excitability state for contextual fear memory formation and precision follow a similar time course during systems memory consolidation.

The impact of interference on memory performance depends on the memory phase

Interference (INT) during early-phase memory has been shown to impair remote memory formation, likely by reallocating these more excitable engram neurons into a new ensemble (Cai et al., 2016). In support of this idea, we found that INT (enriched environment) 1 day following CFC (Early–INT; Fig. 5A) impaired long-term memory performance by decreased freezing during the retrieval (day 30; Fig. 5B). In contrast, the same INT experience during late-phase memory formation (15 days post-CFC; Late–INT) had no impact on remote memory performance (Fig. 5A & B). Freezing levels during CFC were similar between the different groups indicating no differences in memory acquisition (Supplementary Fig. 6A & B).

This data shows the impact of interference on memory formation follows the transient time course of neuron-wide IEP of ACC engram ensembles.

Early-phase excitability manipulation prevents the impact of interference on memory

We then investigated whether the remote memory impairment caused by an early INT experience could be blocked by manipulating the intrinsic excitability during early-phase memory. To address this, we administered CNO for the first seven days following CFC to activate iDREADD on putative ACC engram neurons, exposed the animals to INT on day one, and evaluated remote (30 days post-CFC) memory performance (Fig. 5C). Indeed, this excitability manipulation prevented memory impairment by INT, rescuing the fear expression levels (Fig. 5D). Freezing levels during CFC were similar between the different groups indicating no differences in memory acquisition (Supplementary Fig. 6C & D). The size of the putative engram that supported the acquisition (Suppl. Fig 6E) and retrieval of the associative memory was also similar between groups (Fig. 5E; Supplementary Fig. 6F).

These results further underline the sensitivity of enduring memory formation to changes in the intrinsic excitability of ACC engram ensembles during the early phase of memory consolidation.

DISCUSSION

Growing evidence points to the role of neuronal intrinsic excitability as a complementary plasticity mechanism for the allocation, acquisition, and storage of enduring memories (Chen et al., 2020). Neuron-wide IEP presents a compelling necessary and permissive mechanism for explaining the time-dependent alterations that lead to the permanent storage of memories in engram ensembles of the prefrontal cortex. To fulfill this role, IEP should be triggered by a learning task, specific to the engram ensembles storing these memories, and transient but enduring enough to support other, more permanent storage mechanisms. An increase in the neuron-wide excitability of engram neurons would tune their responsiveness (Frick and Johnston, 2005; Titley et al., 2020; Zhang and Linden, 2003), switching their state into a receptive (or “consolidating”) mode. In this mode, they are more likely to be reactivated by offline coordinated activity of hippocampal-cortical circuits during periods of quiet wakefulness or phases of sleep (Rusu et al., 2024), likely promoting their permanent integration into the engram by driving persisting changes in synaptic plasticity (de Sousa et al., 2019; Diekelmann and Born, 2010; Girardeau and Zugaro, 2011) and strengthening the connections between nascent engram neurons. This increased excitability would also prime the neurons to undergo further plasticity, for instance by altering the amount of associativity and

cooperativity of synaptic inputs required to induce synaptic plasticity. It should last long enough to support permanent storage mechanisms that require repeated activation or are slow to develop over several consecutive days, such as changes in the wiring and strength of synaptic connections (Goto, 2022; Kennedy, 2016). Conversely, neuron-wide IEP would not be a suitable permanent memory storage mechanism, since it would severely lower the storage capacity of neurons compared to one where information is stored in a synapse-specific manner. IEP should therefore return to naïve pre-learning levels once the physical and chemical engram alterations underlying permanent memory storage have been established.

To establish the necessity of this mechanism for long-lasting memory storage, we evaluated learning-induced IEP and used pharmacogenetic manipulations to artificially modulate excitability in those neurons initially tagged during the learning event (nascent engram neurons). We found that not only were these 'tagged' neurons preferentially recruited during remote memory retrieval but also that the intrinsic excitability of these neurons was plastically modified in the days immediately following the learning event. These physiological measures point to a neuron-wide increase in the intrinsic excitability of ACC engram neurons. These changes are transient, lasting several days, and are thus absent in the remote phase of memory storage. How, then, do they contribute to the remote expression of fear memory? This question has dogged discussions of how IEP could contribute to an enduring memory trace (for discussion see (Frick and Johnston, 2005; Hansel and Yuste, 2024; Titley et al., 2020). As we (and others) have speculated, early neuron-wide IEP can set the stage for metaplasticity, for example through gene-expression patterns mediated by ion-channel signaling (Vierra et al., 2021) leading to downstream events that reinforce the communication within the nascent engram network. This is consistent with findings of early tagging events in the prefrontal cortex affecting the remote expression of non-aversive memories (Lesburguères et al., 2011). However, this type of scenario would be computationally limited, and as we and others have demonstrated (Cai et al., 2016), would be vulnerable to additional events that modify the excitability of nascent engram neurons. In a landscape of increased excitability, synaptic inputs to specific neuronal compartments, such as dendritic branches or distal dendrites could create opportunities for localized excitability mechanisms (e.g., as we demonstrated in (Frick et al., 2004). Such localized mechanisms intersect with 'traditional' mechanisms of plasticity such as LTP (Frick et al., 2004; Rosenkranz et al., 2009) and vastly increase the computational compacity for storage of specific memories (Häusser, 2004) due to the vast permutations possible

with such mechanisms. One way that global IEP could contribute during the early to intermediate memory phase is to set the stage for synapse-specific tuning by changes in the intracellular localization and targeting of ion channel complexes. Such changes are known to occur during development (Wilkars et al., 2012) or pathophysiological states (Kv2.1 and epilepsy (Thiffault et al., 2015)), and are often due to the association of pore-forming subunits of an ion channel with accessory subunits that confer properties of localization. The changes reported here are likely due to the orchestrated effect of a spectrum of different ion channel types (Na^+, Ca^{2+}, and K^+ channels) and many of these are susceptible to processes such as phosphorylation or association with accessory subunits that affect their properties (Misonou et al., 2004).

Here we demonstrate changes in the excitability of the L5 PT neurons of the ACC engram network. The results of an overall increased intrinsic excitability are consistent with previous findings with conditioning paradigms, for example, (Weiss et al., 1996). However, it is important to note that this is not the only type of change that is possible, nor the only neuron type present in the ACC engram network. Indeed layer 2/3 pyramidal neurons as well as various interneuron types are also likely targeted by our 'tet-tagging' strategy and it is this complex interplay within the engram network that leads to the behavioral outcomes observed in remote memory. Thus, interventions targeting the excitability of the overall ACC engrams have outcomes that might seem counterintuitive at first consideration but are consistent with the notion of this heterogeneity. Our experiments demonstrate that tuning the excitability of the global ACC engram population has profound consequences for not only the fate of memory formation but also discrimination of specific features (information content) of the conditioning context. Previous accounts have established that increasing initial memory strength at encoding by lengthening the duration of exposure to the aversive context leads to the formation of a larger engram within the hippocampus, resulting in a potentially more richly detailed contextual fear memory being retrieved 24 hours after learning (Leake et al., 2021). Here, by acting on the intrinsic excitability of cortical neurons at the post-encoding stage before the fear engram has matured, we show that it is possible to enhance the subsequent degree of detailed context discrimination. This increased precision correlates with an expansion of fully matured engram cells (see Fig. 6).

Finally, individual memories can be retrieved selectively and accurately even when learning events often overlap with each other. Memories of temporally proximate events are structurally interconnected within overlapping neural ensembles. This overlapping structure can facilitate the linking of these memories, such as that information from the first event is transferred to the second (Cai et al., 2016) or that the second event disrupts the first memory formation by mechanisms of retrospective interference (RI) (Ge et al., 2019). The former is called prospective association (PA), but animal studies showed that fearful events are more likely to be linked retrospectively. Further, PA occurs when there is high similarity between events that are being linked, a condition not met in our experiments. The latter proposes that INT impaired consolidation of CFC memory, through reversal of CFC-induced long-term potentiation (LTP) (Ge et al., 2019), resulting in a failure to retain long-term memory. Pharmacogenetic modulation of IE could therefore influence the process of LTP depotentiation, thereby preserving the original memory.

MATERIALS AND METHODS

Ethical considerations

All animal procedures, including anesthesia and surgery, were conducted under the European guidelines. The experiments were approved by the animal care and use committees of the Université de Bordeaux and of the Institut National de la Santé et de la Recherche Médicale (Inserm) in France. The ethics protocol numbers are 9000 and 12267.

Animals

Double transgenic TetTag mice (Fos-tTA and Fos-EGFP; tetO-lacZ and tTA*) (Jax# 008344) were used for all the experiments that required long-term labeling of putative engram neurons: electrophysiological, DREADD and interference experiments. Single transgenic mice (Fos-tTA and Fos-EGFP) were used for the rest of the experiments. Adult mice of both genders were used for all the behavioral and electrophysiological experiments. As we observed no sex differences in our measures, data from both genders were pooled. Mice aged 8-10 weeks were used for the electrophysiology experiments, while 8-15 week-old mice were used for the rest of all the experiments. Mice were bred in the animal facility of the Neurocentre Magendie, group-housed, and kept at a 12-hour light-dark cycle (light on from 7 am to 7 pm) in temperature-humidity-controlled rooms and with *ad libitum* access to water and doxycycline chow (40 mg

doxycycline/kg). Doxycycline chow was replaced with standard chow (no doxycycline) 60h before fear conditioning to open the temporal window for tagging and provided back immediately following the learning experience.

Viral constructs and stereotaxic surgeries

Two weeks before contextual fear conditioning, the ACC area of TetTag mice brains was stereotactically injected with one of the following adeno-associated viruses (AAVs): AAV1/2-TRE-hM$_3$Dq-mCherry, AAV1/2-TRE-hM$_4$Di-mCherry or AAV1/2-TRE-YFP. Thirty minutes before the surgery, mice received a subcutaneous injection of the analgesic, buprenorphine solution (0.1 mg/kg, AXIENCE SAS). Mice were deeply anesthetized with 4% isoflurane firstly, then placed in a stereotaxic frame, followed by switching to 2% isoflurane for the rest of the surgery. Before the incision of the skin on the skull, mice received a subcutaneous injection of a local anesthetic, lidocaine (0.1 mg/ml, AXIENCE SAS; 0.05-0.1 ml), at the site of the incision. Surgery commenced once the mice displayed no reflexes after paw pinch. Bilateral stereotaxic injections of the AAV were targeted to the ACC using the following coordinates and injection angle: AP +0.9 mm, ML ± 0.75 mm, DV -1.65 mm, 20° from a vertical line. 500 nl of AAV virus was injected into each site at a rate of 100 nl/min. The needle was slowly removed 5 min after completion of the injection. Mice were given a two-week post-surgery recovery period before commencing experiments. The plasmids were kindly provided by S. Togenawa (MIT), and the adeno-associated virus was produced in Neurocentre Magendie institute.

Behavioral testing

Contextual fear conditioning

Before the behavioral training, mice were habituated in a waiting room and handled daily (10–20 min) for five consecutive days. Contextual fear conditioning (CFC) consisted of a 3-min free-exploring phase of the mice to the conditioning chamber (context A, scented with 70% ethanol), followed by five 2 s-long foot shocks (intensity 0.7 mA) with a shock interval of 30 s. Context A was a grey plastic chamber (26 cm in length, 25 cm in-depth, 18 cm in height, Imetronic Company, Pessac, France) with a metal grid floor to deliver electric shocks and a transparent Perspex door. After the shocks, the animals remained in the chamber for an additional 30 seconds. A control group of animals (CTX) was exposed to context A for the same amount of time (five minutes and

40 seconds in total) but without receiving any foot shocks, also scented with 70% ethanol. For memory recall, mice were re-exposed to the conditioning chamber (context A) for 3 min without receiving foot shocks, or to context B (chamber with an additional white, prism-like box with a plastic floor that was shaped like a triangle and contained no metal grids) in the same room (see Supplementary Table 3 for detailed comparison of contexts A and B). To evaluate the strength of fear memory during different phases of memory formation, we assessed the mice's freezing time in a given context (A or B). The freezing behavior was considered as the absence of any movement, except for respiratory-related movement (Fanselow, 1990; Paylor et al., 1994).

Freezing time during memory recall was manually counted by two independent experimenters who were blind to the experimental conditions. The percentage of freezing was calculated as the measured freezing time divided by the three minutes of the retrieval period. We also calculated the freezing time during the 30 seconds following the last shock of CFC (% freezing after learning) as the basal freezing level for every mouse. Delta freezing (Δ freezing) was calculated as follows: Δ freezing = (% freezing during retrieval) – (% freezing after learning).

Supplementary Table 3. Comparison of context A and context B

	Context A	Context B
Photo	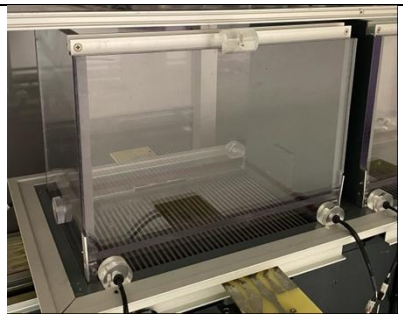	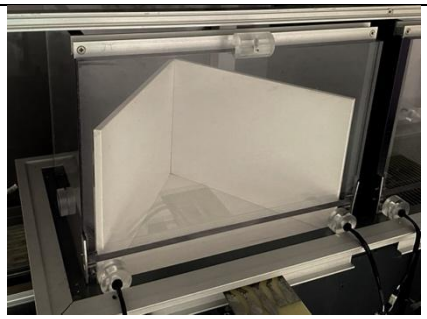
Size	L:26 cm, D: 24cm, H:18 cm	L:24 cm, D:17 cm, H:15 cm
Floor	Metal grid, rectangular	Plastic pad, triangle
Wall	Grey plastic wall with one transparent door	White plastic wall with one transparent door
Oder	70% ethanol	No ethanol
Light	Ambient light	Ambient light

Pharmacogenetic manipulation

To modulate the intrinsic excitability of neuronal ACC engram ensembles that were transduced with AAV1/2-TRE-hM_3Dq-mCherry (excitatory DREADD, eDREADD) or AAV1/2-TRE-hM_4Di-mCherry (inhibitory DREADD, iDREADD), mice received Clozapin-N-oxide (CNO) or vehicle (saline, Sal) via intraperitoneal (*i.p.*) injection twice a day. To modulate intrinsic excitability during the early stages of memory consolidation, the first CNO/vehicle *i.p.* injection was administered 6 hours after the CFC and continued daily for the subsequent seven days. To alter the excitability of engram ensembles during the late memory consolidation, mice received the first CNO/vehicle *i.p.* injection on day 14 after the CFC and then for the following seven consecutive days (until day 21 following CFC). Injections were delivered between 9 and 10 a.m. and 3 and 4 p.m. on a given day. Mice were returned to their cages immediately after *i.p.* injection.

CNO (TOCRIS) was dissolved in DMSO (Sigma-Aldrich) at a stock concentration of 5 mg/ml and stored at -20°C. Aliquots of CNO stock solution were thawed before the injections and diluted to a final concentration of 0.5 mg/ml with a 0.9% NaCl solution. DMSO was diluted in the same manner and served as control (vehicle). CNO (vehicle) was injected *i.p.* at 5 mg/kg body weight.

We verified the expression of the DREADD receptors within the ACC area of interest by visualizing the mCherry signal in brain slices using confocal microscopy (described below). Only mice with mCherry expression at the appropriate ACC area were considered for histological, behavioral, and statistical analyses.

Memory interference protocol

On day 1 (early memory interference, early INT) or day 15 (late memory interference, late INT) following CFC, individual mice were either allowed to explore a novel environment for 2 h (interference group, INT) or stayed in their home cage (no-INT group). This novel environment consisted of a cage twice the size of the home cage, covered with black paper, with only one transparent side to see the wall cues. Toys were placed inside the cage and rearranged every 20 minutes to stimulate exploratory behavior. In addition, mice had access to a running wheel for an hour. Water and doxycycline food was available for the duration of the whole experiment. The influence of interference on memory recall was assessed 30 days after CFC by placing mice in the same context where they were conditioned (context A) for 3 minutes.

To probe how pharmacogenetic modulation of the intrinsic excitability of ACC engram neurons alters the INT-induced impairment of memory formation, animals were injected with AAV1/2-TRE-hM$_4$Di-mCherry into the ACC two weeks before CFC. Mice of the INT group were randomly divided into two subgroups, one receiving *i.p.* CNO injections (INT_CNO) and the other *i.p.* vehicle injections (INT_Saline) for seven days each during either the early- or remote phase of memory consolidation (see above). The control group (no-INT_Saline) received vehicle injections during the same 7-day period and stayed in their home cage. Memory retrieval was performed for all three groups (INT_CNO, INT_Sal, no-INT_Saline) 30 days after CFC in Context A.

Electrophysiology

ACC slice preparation

Mice were sacrificed for electrophysiological recordings 1-3 days or 15-17 days following the behavioral session (CFC or CTX) without memory recall. Mice were injected with an analgesic, deeply anesthetized with isoflurane, and intracardially perfused with ice-cold (4°C) cutting solution (Supplementary Table 4) once the mice displayed no reflexes after paw pinch. Following the perfusion, mice were decapitated, heads were immersed in the ice-cold cutting solution, and the brains were rapidly removed. Coronal slices of 300 µm were cut using a vibratome (Vibratome 3000 Plus, Sectioning Systems) and gently transferred to an incubating chamber filled with artificial cerebrospinal fluid (aCSF) resting solution (Supplementary Table 4). Following 40 min of incubation at 37°C, slices were transferred to a second incubation chamber containing aCSF recording solution at room temperature (~ 23°C) (Supplementary Table 4). Brain slices were allowed to recover for at least one hour before electrophysiology recordings. All the solutions were saturated with carbogen (95% O_2, 5% CO_2), the pH adjusted to 7.32–7.40, and the osmolarity adjusted to 295–310 mOsm.

Ingredients (mM)	**Cutting solution**	**aCSF resting solution**	**aCSF recording solution**	**Internal solution**
NaCl	-	124	124	-

NMDG	93	-	-	-
KCl	2.5	2.5	2.5	4
$NaH_2PO_4 \cdot H_20$	1.25	1.25	1.25	-
$NaHCO_3$	30	24	24	-
HEPES	20	5	5	10
D-Glucose	35	12.5	12.5	-
Thiourea	2	-	-	-
Na-ascorbate	5	1	-	-
Na-pyruvate	3	4	-	-
$CaCl_2 \cdot 2H_2O$	0.5	2	2	-
$MgSO_4 \cdot 7H_2O$	10	2	2	-
K-gluconate	-	-	-	135
Phospocreatine-Na	-	-	-	10
Na-GTP	-	-	-	0.3
Mg-ATP	-	-	-	4

Supplementary Table 4. Composition of external and pipette solutions

Whole-cell patch-clamp recordings

Following the behavioral protocol, mice were randomly assigned to the 1-3-day and 15-17-day groups for electrophysiological experiments. Layer 5 thick-tufted pyramidal neurons within acute ACC slices were selected for whole-cell recordings using an upright microscope (Zeiss Examiner) equipped with a 63X/1.0 NA water immersion objective (Zeiss) and an IR-Dodt contrast system. An Evolve 512 EMCCD Camera (Photometrics) combined with an LED system (560 nm; Colibri, Zeiss) and a Filter Set 62 HE (Zeiss) was used for visualizing YFP-expressing putative ACC engram neurons. For whole-cell recordings, borosilicate glass capillaries (Harvard Instruments, GC150F-7.5) were pulled using a PC-100 vertical puller (NARISHIGE Group). The pipettes were filled with internal recording solution (Supplementary Table 2), and the open-tip resistance ranged from 5 to 7 MΩ. The osmolarity of the internal solution containing 0.3% biocytin (Reference: 90055, Biotium) was adjusted to 290 mOsm, and the pH was set to be 7.30. Solution was stored at -20℃ and kept on ice before use. The recording chamber of the electrophysiology setup was perfused with oxygenated aCSF at a temperature of 32℃ during the whole experiment.

Recordings were performed in the bridge-mode using a BVA-700C amplifier (Dagan, USA). Data was low-pass filtered at 3 kHz and sampled at 20 kHz using an ITC-18 (InstruTECH) Data Acquisition Interface and AxoGraph X software (version 1.7.6). Bridge resistance and capacitance were compensated and monitored during the recording period. Cells were discarded if the resting membrane potential was depolarized above -50 mV. All electrophysiological properties were measured in the bridge-mode.

To measure the intrinsic properties of ACC neurons, recordings were performed in the presence of the following blockers of glutamatergic and GABAergic synaptic transmission: AMPA receptor antagonist, NBQX (disodium salt, TOCRIS; concentration: 3uM in aCSF), NMDA receptor antagonist, DL-AP5 (TOCRIS; 50uM), and $GABA_A$ receptor antagonist, SR 95531 (hydrobromide, TOCRIS; 10uM).

Morphological reconstruction of recorded neurons

After electrophysiological recordings, the brain slices containing the biocytin-filled recorded neurons were fixed in 4% PFA for two hours and then transferred to 0.1 M PBS solution at 4°C for longer preservation. Brain slices were washed three times with 0.1 M PBS and then submerged for two hours at room temperature with a 0.7% Triton X-100 solution (EUROMEDEX). Slices were incubated with a solution that contained Streptavidin-Alexa 555 (1:1000, Thermo Fisher, Reference: S21318) and 0.3% Triton X-100 for three hours. The brain slices were then washed with 0.1 M PBS three times and incubated with DAPI (1:10000, Sigma-Aldrich) for five minutes. Brain slices were mounted on microscope slides using Mowiol-Dabco and thin coverslips.

Confocal microscopy was used to determine the recorded neurons (YFP+/Alexa 555+ positive neurons). The distances of the recorded neurons to the pia and the beginning of layer 2 were also measured to define the layer localization of the neurons. The morphology of soma and dendrites was reconstructed with Neurolucida, and only *post hoc* identified layer 5 tick-tufted pyramidal neurons were included for analysis.

Electrophysiological data analysis

Electrophysiological data were analyzed using AxoGraph X and customized Python analysis routines. The resting membrane potential (RMP) was measured 3 minutes after whole-cell access

and switching to the bridge mode to allow for the cells to stabilize. The input resistance was measured as the average (five trials) steady-state voltage deflection to a -20 pA current step (800 ms duration). Rheobase and the number of action potentials (AP) as a function of current were determined by injecting a series of depolarizing current steps of increasing amplitude (between 20 and 300 pA, 20 pA increments, 800 ms duration). The rheobase was defined as the minimum amount of current necessary to evoke the first AP. The first AP within a train of 4-5 APs was analyzed for AP threshold (dV/dt exceeding 10mV/ms, in mV), AP amplitude (from RMP to peak amplitude, mV), AP half-width (duration at half-distance between AP threshold and amplitude, ms), and maximum rate of rise (dV/dt, mV/ms). The inter-spike interval (ISI, ms) was measured between the first two and the last two APs within a train of 4-5 APs, and the adaptation index was measured as follows: (first ISI) / (last ISI). The % of sag response was calculated using hyperpolarizing current injections as follows: (voltage difference between steady-state and the minimum of the hyperpolarization) / (voltage difference between the RMP and the minimum of the hyperpolarization) * 100 (in %). The membrane time constant (ms) was calculated from voltage responses to alternating depolarizing and hyperpolarizing 400 pA 1-s-long current pulses. It was then calculated as the slow component of a double-exponential fit of the average voltage decay in both the depolarizing and hyperpolarizing directions. The medium afterhyperpolarization (mAHP) was measured as the minimum (relative to RMP) 50-100 ms following the last AP within a train of 5 APs (2 ms pulses, 2 nA) evoked at frequencies ranging from 20 to 120 Hz (at 20 Hz intervals) and 200 Hz. The slow AHP (sAHP) was measured as the minimum following the last AP in the train of 15 APs induced by 2 nA pulses at 20 Hz for 2s.

Immunohistochemistry and imaging

Sacrifice and slice preparation

90 min after the behavior, mice were deeply anesthetized by 4% isoflurane and intraperitoneally injected with a solution containing 400 mg/ml of pentobarbital (Exagon, Med'Vet), 0.1 mg/ml of lidocaine (Lidor, AXIENCE SAS) in 0.9% NaCl solution. The injection dose was 0.1 ml per 10 grams weight for the mice. Mice were then transcardially perfused with 0.1 M phosphate-buffered saline (PBS) followed by 4% cold paraformaldehyde (PFA). Mice of the home-cage group, which did not undergo any behavioral procedure, were perfused on the same day. Brains were dissected

and postfixed overnight in 4% paraformaldehyde, then sliced into 50-µm coronal sections using a vibratome.

Immunohistochemistry staining

Brain slices were washed three times with 0.1 M PBS for 10 minutes each, and then blocked for one hour at room temperature with the following blocking solution: 5% BSA (EUROMEDEX) mixed with 0.3% Triton X-100 (EUROMEDEX). To enhance the EGFP signal, slices were incubated with anti-GFP rabbit polyclonal antibody Alexa-488 (1:1000, Thermo Fisher, Reference: A21311) overnight at 4°C in a solution containing 1% BSA and 0.3% Triton X-100. The following day, slices were washed three times with 0.1 M PBS for 10 minutes each and incubated with DAPI (1:10000, Sigma-Aldrich) for 5 minutes. After being washed once with 0.1 M PBS, the brain slices were mounted using Mowiol-Dabco and thin coverslips on microscope slides.

Confocal image acquisition and analysis

Fluorescence images were acquired using a Zeiss LSM700 confocal microscope equipped with a Leica 20X/1.3 NA oil immersion lens provided by the Bordeaux Imaging Centre (BIC). Two to three coronal slices per mouse were imaged at multiple depths along the z-axis (z-stack of 32 µm with 4 µm interval steps). Imaris software (version 9.6.2) enabled the reconstruction of a 3-dimensional model from confocal microscopy images. Cell counting analysis was performed using Imaris and ImageJ-Fiji software (provided by BIC). The area of the anterior cingulate cortex was selected and measured with ImageJ-Fiji. The number of mCherry-positive, EGFP-positive, co-localized (mCherry+/GFP+), and DAPI-positive neurons were counted and expressed as density in mm2 ((#cells/area size (um2))*1000000). Image acquisition and analysis were performed blind to the experimental conditions.

Statistical Analysis

Statistical tests were performed using Prism 10.0 (GraphPad). The normality distribution of the data was examined using the D'Agostino-Pearson omnibus normality test. If the data was normally distributed, an unpaired Student's *t-test*, a one-way ANOVA, or a two-way ANOVA test was performed. Otherwise, nonparametric tests were performed. When performing the ANOVA test,

the standard deviation of the data set was examined. To identify outliers ROUT (Q=0.1%) method was used. The post-hoc multiple comparisons were performed using the Tukey or Sidak test. Data are displayed as mean ± SEM. The significance threshold was set at α=0.05 (NS, * *P<0.05*, ** *P<0.01*, ***P<0.001*, **** *P<0.0001*).

Figures and Figure legends

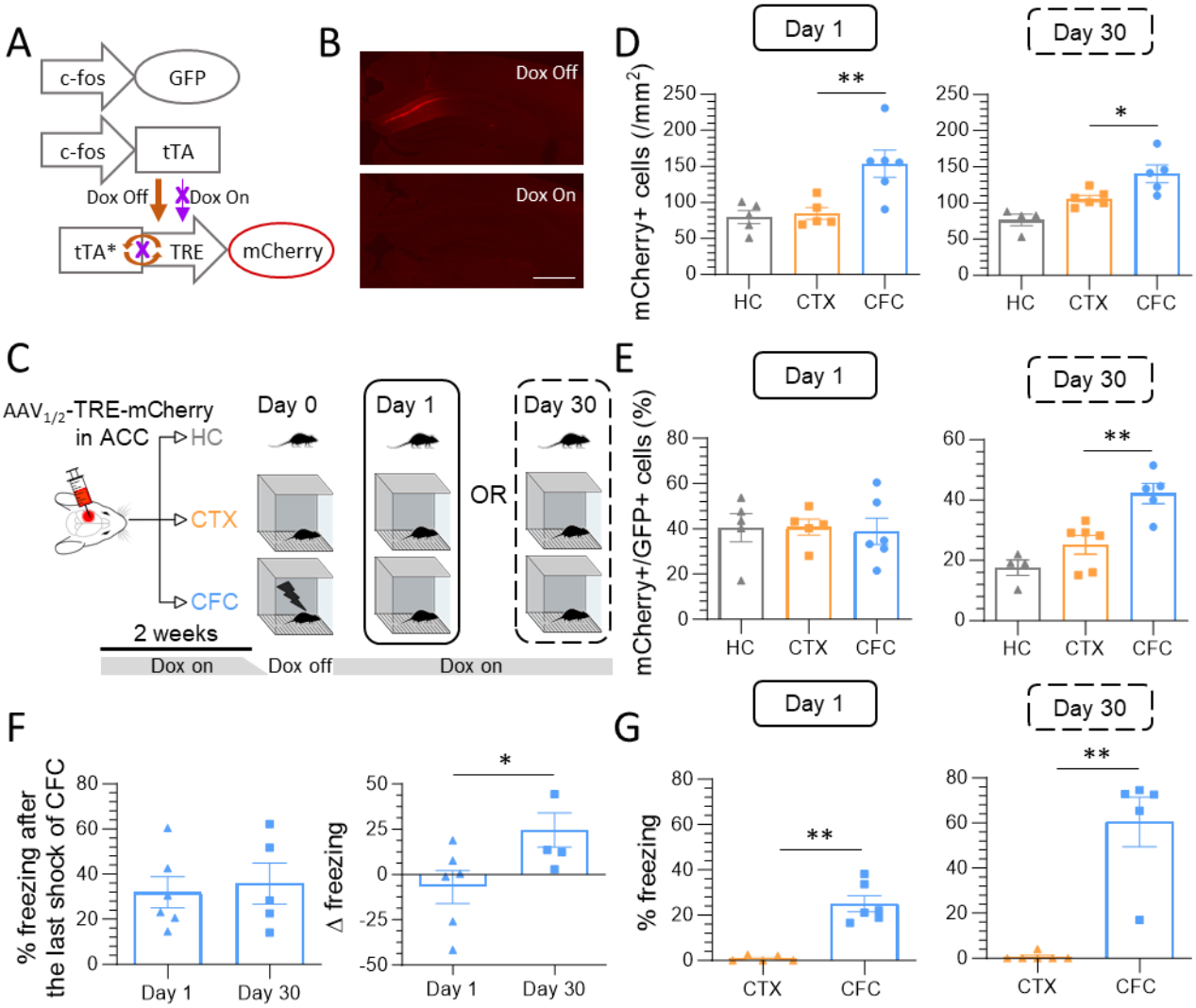

Figure 1. ACC engram ensembles are tagged by learning and reactivated during remote memory expression) **A.** Strategy for lasting neuronal tagging of engram neurons using the Tet-tag mouse together with $AAV_{1/2}$-TRE-mCherry. GFP is expressed with a short half-life under the control of the *c-fos* promotor. **B.** Representative images show that mCherry-tagging only occurred in the absence of doxycycline (Dox Off). Scale bar 700 µm. **C.** Experimental design: CFC (contextual fear conditioning), CTX (context only), and HC (home cage) were performed on separate groups of mice during the Dox-off phase and memory retrieval was tested either 1 day or 30 days later. **D.** ACC neurons were strongly engaged during CFC (mCherry+ neurons) and this tag was stably expressed for at least 30 days. **E.** Reactivation of tagged ACC neurons by memory retrieval during the early or remote phase of memory consolidation was expressed as the ratio of mCherry+ to GFP+ neurons. **F.** CFC leads to the formation of a long-

lasting (>30 days post-CFC) fear memory, expressed as a significant increase in the difference in freezing (Δ freezing, right) time during retrieval and freezing after the last shock (left). **G.** Freezing behavior as an indicator of associative memory is expressed following CFC but not in the CTX group. Data points are individual mice with mean ± SEM. Statistical significance was calculated using one-way ANOVA (D-E), Unpaired t-test (F), or Mann-Whitney test (G) *P<0.05, **P < 0.01.

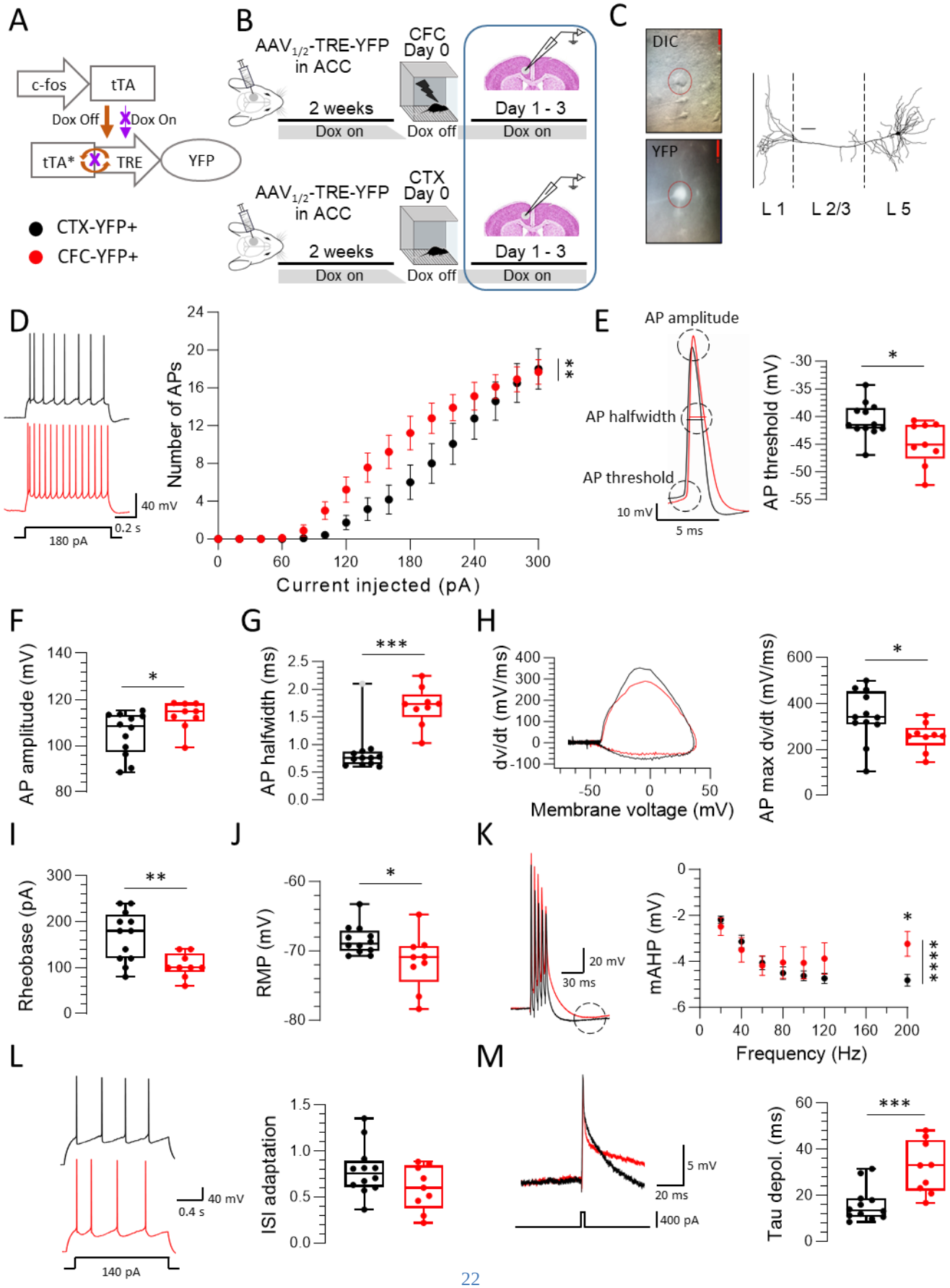
A
c-fos
tTA
Dox Off
Dox On
tTA*
TRE
YFP
CTX-YFP+
CFC-YFP+
B
AAV1/2-TRE-YFP in ACC
CFC Day 0
2 weeks
Dox on
Dox off
Day 1 - 3
Dox on
AAV1/2-TRE-YFP in ACC
CTX Day 0
2 weeks
Dox on
Dox off
Day 1 - 3
Dox on
C
DIC
YFP
L 1
L 2/3
L 5
D
40 mV
0.2 s
180 pA
Number of APs
Current injected (pA)
E
AP amplitude
AP halfwidth
AP threshold
10 mV
5 ms
AP threshold (mV)
F
AP amplitude (mV)
G
AP halfwidth (ms)
H
dv/dt (mV/ms)
Membrane voltage (mV)
AP max dv/dt (mV/ms)
I
Rheobase (pA)
J
RMP (mV)
K
20 mV
30 ms
mAHP (mV)
Frequency (Hz)
L
40 mV
0.4 s
140 pA
ISI adaptation
M
5 mV
20 ms
400 pA
Tau depol. (ms)

Figure 2. Contextual fear conditioning triggers IEP in ACC engram ensembles. **A.** Strategy for tagging ACC engram neurons (YFP expression). **B.** Experimental design: whole-cell patch-clamp recordings were performed from YFP+ neurons 1-3 days post-CFC or post-CTX. **C.** Representative images (DIC and fluorescence image) during recording, and Neurolucida reconstruction, of a YFP+-L5-PT pyramidal neuron. Scale bar 50 um. **D-M.** Analysis for n=9 YFP+ cells (CFC group) and n=12 YFP+ cells (CTX group). **D.** ***Left***: Example traces of action potentials (APs) induced by a 180-pA current injection for a CFC and a CTX neuron. ***Right***: Significant increase in the number of APs as a function of injected current in CFC neurons. **E.** ***Left*****:** Example traces of single APs from a CFC and a CTX neuron, illustrating differences in the threshold, amplitude, and half-width. ***Right***: More hyperpolarized AP threshold in CFC neurons. Increase in AP amplitude (**F**) and AP half-width (**G**) ***Left*****:** Example traces for AP upstroke velocity (max dv/dt). ***Right:*** Decreased in max dv/dt. **I**. Reduction in rheobase. **J**. More hyperpolarized resting membrane potential (RMP). **K.** ***Left:*** Example traces of medium after-hyperpolarization (mAHP) from a 5-AP-train at 200 Hz. ***Right:*** Significant reduction in mAHP amplitude for high frequencies. **L.** ***Left:*** Example traces for AP adaptation during a train of 4 APs. ***Right:*** Trend for reduced inter-spike interval (ISI) adaptation in CFC-YFP+ neurons. **M.** ***Left:*** Example traces of membrane potential time constant (Tm) following a brief depolarization. Increase in Tm. Data points are individual cells with median, lower and upper quartiles, and minimum and maximum data values. Statistical significance was calculated using repeated measures of two-way ANOVA followed by Šídák's multiple comparisons test (D), Mixed-effects model when there were missing values (K) or Unpaired t-test (E-J, L, M), *P<0.05, **P < 0.01, ***P < 0.001, ****P < 0.0001.

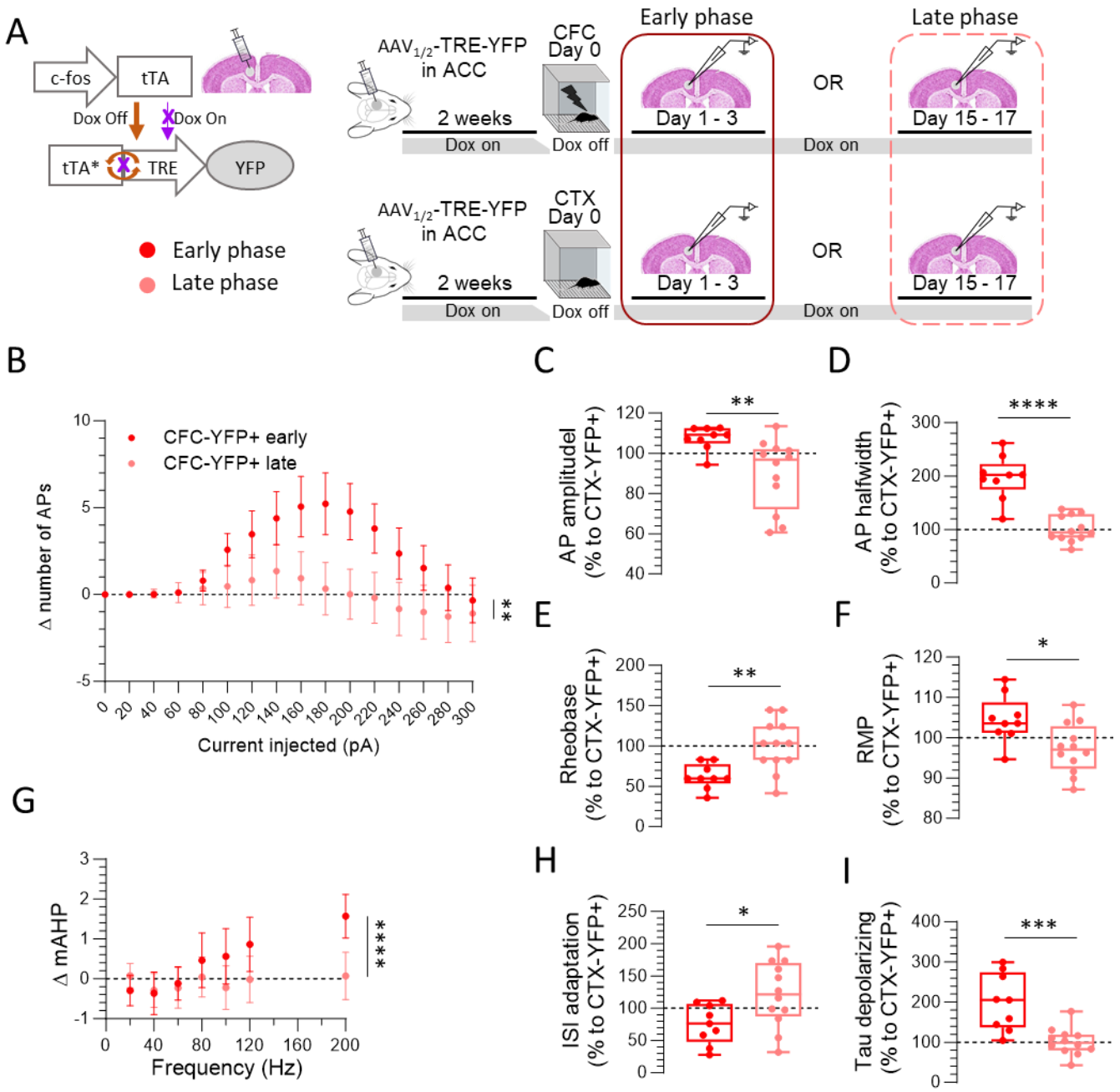

Figure 3. The transient nature of IEP of the ACC engram neurons.

A. ***Left*:** Strategy for tagging of ACC engram neurons (YFP expression). ***Right:*** Experimental design. Whole-cell patch-clamp recordings were performed from tagged (YFP+) L5 pyramidal neurons either during early-phase (1-3 days post-CFC) or remote-phase (15-17 days post-CFC) memory consolidation. Data are normalized to values from control cells (CTX-YFP+) at the respective phases. **B-I.** Analysis for n=9 cells (early-phase memory) and n=12 cells (remote-phase memory). Significant differences were found for the number of APs (presented as Δ: difference in the values between CFC-YFP+ and CTX-YFP+) **(B)**, AP amplitude **(C)**, AP halfwidth **(D)**, rheobase **(E)**, RMP **(F)**, mAHP amplitude, presented as Δ: difference in the values between CFC-YFP+ and CTX-YFP+ **(G)**, ISI adaptation **(H)**, and Tau **(I)**. Data points are individual cells with median, lower and upper quartiles, and minimum and maximum data values. Statistical significance was calculated using repeated measures of two-way ANOVA followed by Šídák's multiple comparisons tests (B), mixed-effects model when there were missing values (G) or unpaired t-test (C-F, H, I), *P<0.05, **P < 0.01, ***P < 0.001, ****P < 0.0001.

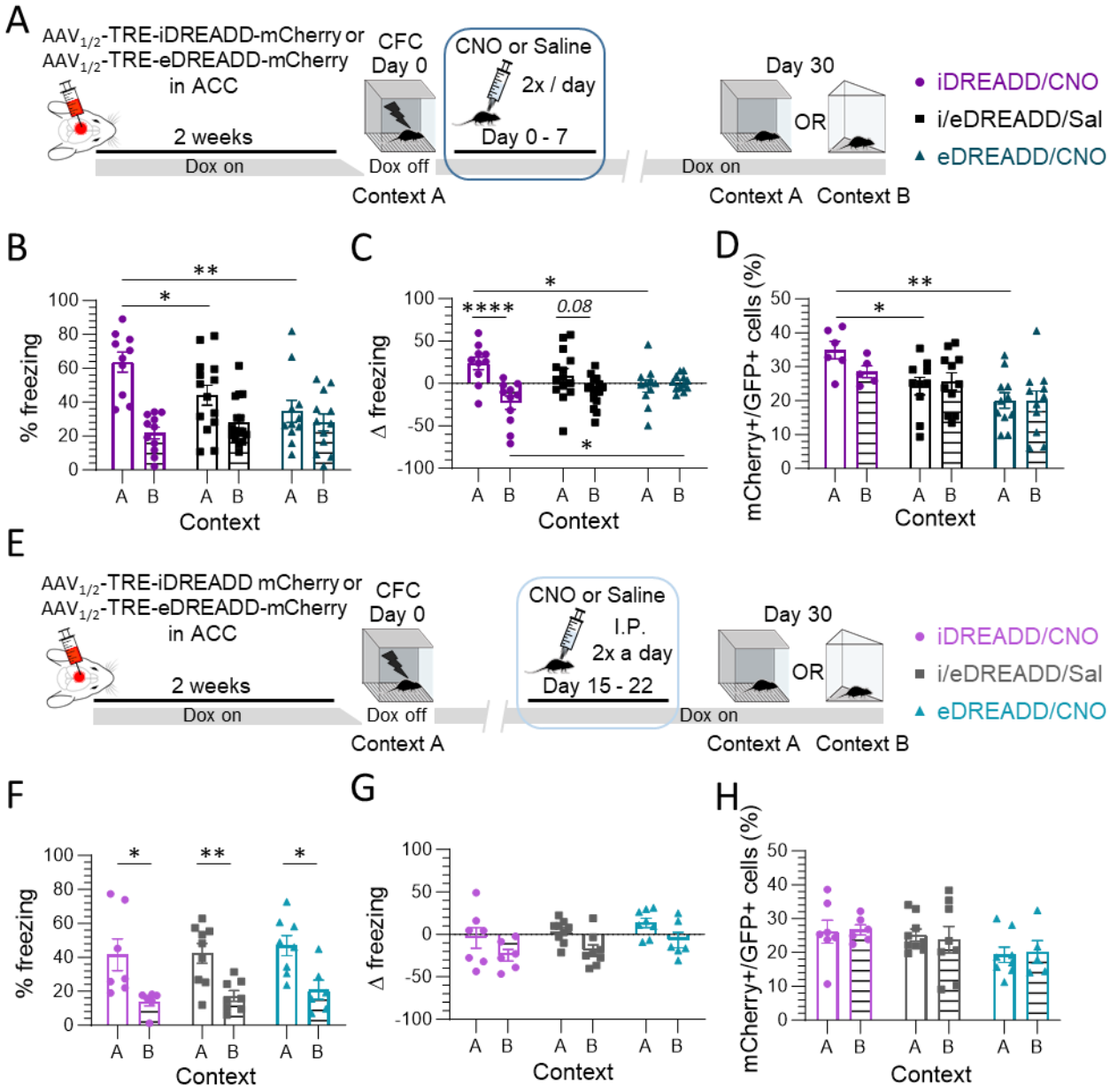

Figure 4. Modulating the intrinsic excitability of ACC engram neurons during its sensitive phase determines the formation and precision of remote fear memories

A. Experimental design: Testing the consequence of manipulating the intrinsic excitability of ACC engram ensembles during early-phase memory consolidation for the outcome and context-precision of remote (day 30 post-CFC) fear memories. **B.** Results are presented for the three groups (iDREADD/CNO, eDREADD/CNO, i/eDREADD/Sal) as the % of time spent freezing during memory retrieval. **C.** Results are presented as Δ freezing (difference in the % of freezing between retrieval and after the last shock during memory acquisition). **D.** % of reactivated tagged ACC engram neurons following remote memory retrieval (mCherry+/GFP+ cells). **E.** Experimental design: Same as in **(A)**, but excitability manipulation during remote-phase memory consolidation. **F-G.** No impact of this manipulation on remote fear expression **(F)** and Δ freezing **(G)** in either the iDREADD/CNO or eDREADD/CNO mice compared to the i/eDREADD/Sal group. **H.** % of reactivated tagged ACC engram neurons during remote memory retrieval. Data points are individual mice with mean ± SEM. Statistical significance was calculated using two-way ANOVA followed by Tukey/Šídák's multiple comparisons test (B-G, F-H), *P<0.05, **P < 0.01, ****P < 0.0001.

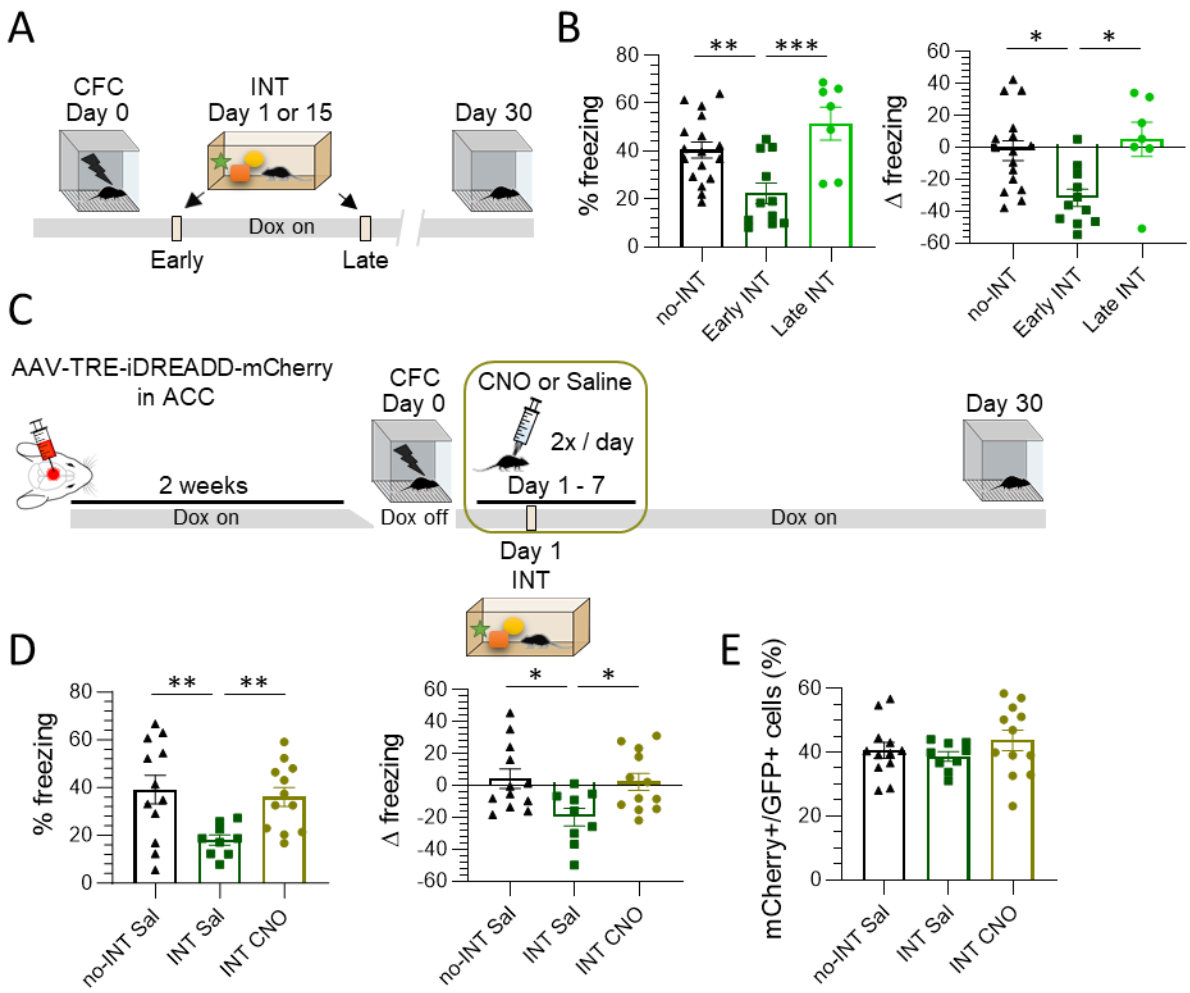

Figure 5. Early-phase manipulation of the intrinsic excitability state of ACC engram neurons prevents memory impairment caused by interference

A. Experimental design for evaluating remote memory expression following interference (enriched environment): Mice underwent interference protocol one day or 15 days post-CFC. **B.** Difference in fear expression (% freezing and Δ freezing) between the three groups (no interference, early-phase interference, late-phase interference). **C.** Experimental design: iDREADD-expressing ACC engram ensembles were injected with CNO for 7 days post-CFC, with INT occurring 24h following CFC and memory retrieval on day 30. **D.** Difference in fear expression between the three groups. **E.** Percentage of reactivated (mCherry+/GFP+ cells) ACC engram neurons during remote retrieval. Data points are individual mice with mean ± SEM. Statistical significance was calculated using Unpaired t-test (B, D, E), *P<0.05, **P < 0.01, ***P < 0.001.

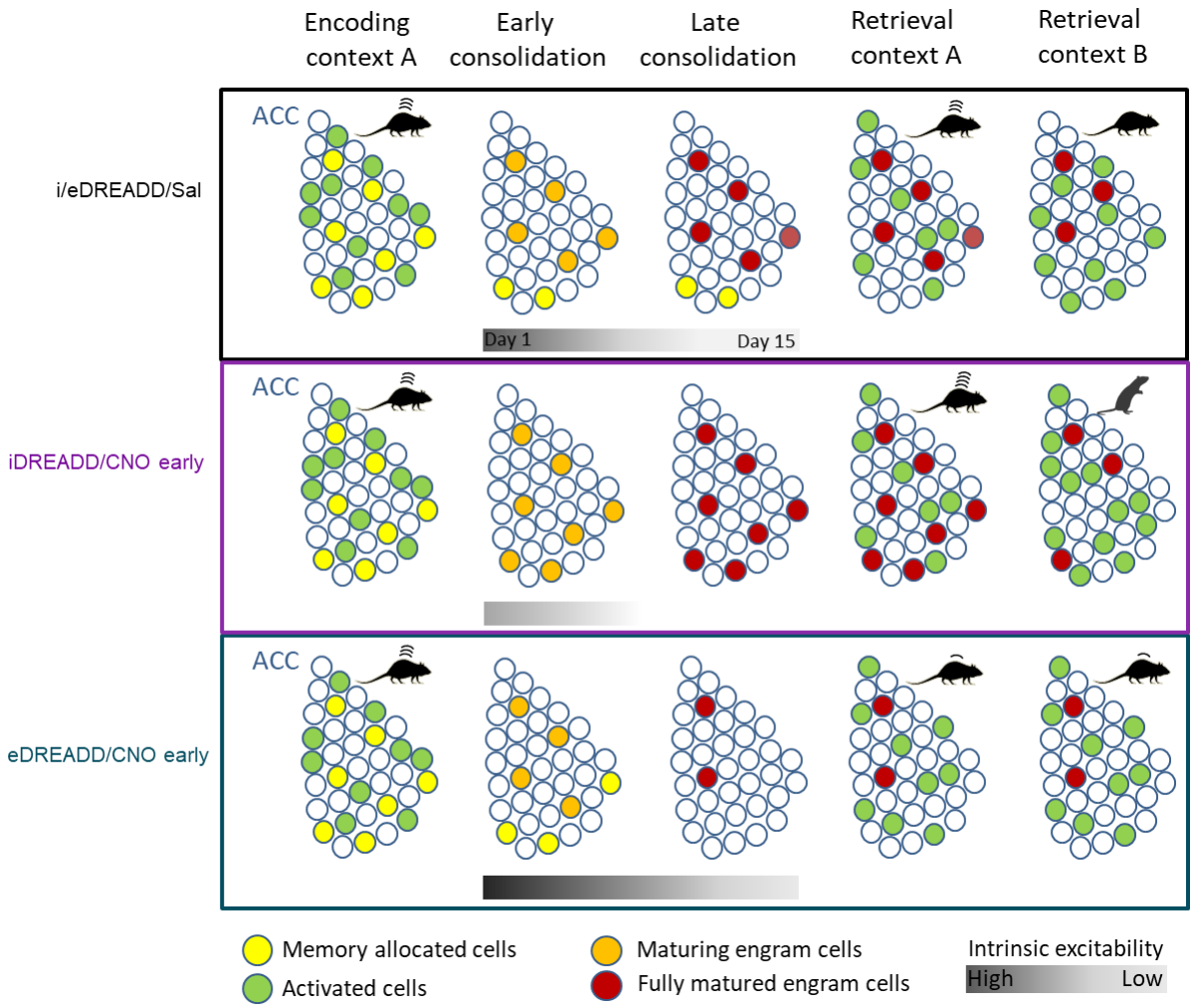

Figure 6. Diagram proposing the mechanisms involving intrinsic excitability changes for long-term memory engram consolidation.

5

References and Notes

Abraham, W.C., Bear, M.F., 1996. Metaplasticity: the plasticity of synaptic plasticity. Trends Neurosci. 19, 126–130. https://doi.org/10.1016/s0166-2236(96)80018-x

Bero, A.W., Meng, J., Cho, S., Shen, A.H., Canter, R.G., Ericsson, M., Tsai, L.-H., 2014. Early remodeling of the neocortex upon episodic memory encoding. Proc. Natl. Acad. Sci. 111, 11852–11857. https://doi.org/10.1073/pnas.1408378111

Cai, D.J., Aharoni, D., Shuman, T., Shobe, J., Biane, J., Song, W., Wei, B., Veshkini, M., La-Vu, M., Lou, J., Flores, S., Kim, I., Sano, Y., Zhou, M., Baumgaertel, K., Lavi, A., Kamata, M., Tuszynski, M., Mayford, M., Golshani, P., Silva, A.J., 2016. A shared neural ensemble links distinct contextual memories encoded close in time. Nature 534, 115–118. https://doi.org/10.1038/nature17955

Chen, L., Cummings, K.A., Mau, W., Zaki, Y., Dong, Z., Rabinowitz, S., Clem, R.L., Shuman, T., Cai, D.J., 2020. The role of intrinsic excitability in the evolution of memory: significance in memory allocation, consolidation, and updating. Neurobiol. Learn. Mem. 173, 107266. https://doi.org/10.1016/j.nlm.2020.107266

de Sousa, A.F., Cowansage, K.K., Zutshi, I., Cardozo, L.M., Yoo, E.J., Leutgeb, S., Mayford, M., 2019. Optogenetic reactivation of memory ensembles in the retrosplenial cortex induces systems consolidation. Proc. Natl. Acad. Sci. 116, 8576–8581. https://doi.org/10.1073/pnas.1818432116

Diekelmann, S., Born, J., 2010. The memory function of sleep. Nat. Rev. Neurosci. 11, 114–126. https://doi.org/10.1038/nrn2762

Dixsaut, L., Gräff, J., 2021. The Medial Prefrontal Cortex and Fear Memory: Dynamics, Connectivity, and Engrams. Int. J. Mol. Sci. 22, 12113. https://doi.org/10.3390/ijms222212113

Frankland, P.W., Bontempi, B., 2005. The organization of recent and remote memories. Nat. Rev. Neurosci. 6, 119–130. https://doi.org/10.1038/nrn1607

Frankland, P.W., Bontempi, B., Talton, L.E., Kaczmarek, L., Silva, A.J., 2004. The Involvement of the Anterior Cingulate Cortex in Remote Contextual Fear Memory. Science 304, 881 LP – 883. https://doi.org/10.1126/science.1094804

Frick, A., Johnston, D., 2005. Plasticity of dendritic excitability. J. Neurobiol. 64, 100–115. https://doi.org/10.1002/neu.20148

Frick, A., Magee, J., Johnston, D., 2004. LTP is accompanied by an enhanced local excitability of pyramidal neuron dendrites. Nat. Neurosci. 7, 126–135. https://doi.org/10.1038/nn1178

Ge, M., Song, H., Li, H., Li, R., Tao, X., Zhan, X., Yu, N., Sun, N., Lu, Y., Mu, Y., 2019. Memory Susceptibility to Retroactive Interference Is Developmentally Regulated by NMDA Receptors. Cell Rep. 26, 2052-2063.e4. https://doi.org/10.1016/j.celrep.2019.01.098

Girardeau, G., Zugaro, M., 2011. Hippocampal ripples and memory consolidation. Curr. Opin. Neurobiol., Behavioural and cognitive neuroscience 21, 452–459. https://doi.org/10.1016/j.conb.2011.02.005

Goto, A., 2022. Synaptic plasticity during systems memory consolidation. Neurosci. Res. 183, 1–6. https://doi.org/10.1016/j.neures.2022.05.008

Hansel, C., Yuste, R., 2024. Neural ensembles: role of intrinsic excitability and its plasticity. Front. Cell. Neurosci. 18, 1440588. https://doi.org/10.3389/fncel.2024.1440588

Häusser, M., 2004. Storing memories in dendritic channels. Nat. Neurosci. 7, 98–100. https://doi.org/10.1038/nn0204-98

Kennedy, M.B., 2016. Synaptic Signaling in Learning and Memory. Cold Spring Harb. Perspect. Biol. 8, a016824. https://doi.org/10.1101/cshperspect.a016824

Kitamura, T., 2017. Driving and regulating temporal association learning coordinated by entorhinal-hippocampal network. Neurosci. Res. 121, 1–6. https://doi.org/10.1016/j.neures.2017.04.005

Leake, J., Zinn, R., Corbit, L.H., Fanselow, M.S., Vissel, B., 2021. Engram Size Varies with Learning and Reflects Memory Content and Precision. J. Neurosci. Off. J. Soc. Neurosci. 41, 4120–4130. https://doi.org/10.1523/JNEUROSCI.2786-20.2021

Lesburguères, E., Gobbo, O.L., Alaux-Cantin, S., Hambucken, A., Trifilieff, P., Bontempi, B., 2011. Early Tagging of Cortical Networks Is Required for the Formation of Enduring Associative Memory. Science 331, 924 LP – 928. https://doi.org/10.1126/science.1196164

Misonou, H., Mohapatra, D.P., Park, E.W., Leung, V., Zhen, D., Misonou, K., Anderson, A.E., Trimmer, J.S., 2004. Regulation of ion channel localization and phosphorylation by neuronal activity. Nat. Neurosci. 7, 711–718. https://doi.org/10.1038/nn1260

Rashid, A.J., Yan, C., Mercaldo, V., Hsiang, H.-L., Park, S., Cole, C.J., De Cristofaro, A., Yu, J., Ramakrishnan, C., Lee, S.Y., Deisseroth, K., Frankland, P.W., Josselyn, S.A., 2016. Competition between engrams influences fear memory formation and recall. Science 353, 383–387. https://doi.org/10.1126/science.aaf0594

Rosenkranz, J.A., Frick, A., Johnston, D., 2009. Kinase-dependent modification of dendritic excitability after long-term potentiation. J. Physiol. 587, 115–125. https://doi.org/10.1113/jphysiol.2008.158816

Roy, D.S., Park, Y.-G., Kim, M.E., Zhang, Y., Ogawa, S.K., DiNapoli, N., Gu, X., Cho, J.H., Choi, H., Kamentsky, L., Martin, J., Mosto, O., Aida, T., Chung, K., Tonegawa, S., 2022. Brain-wide mapping reveals that engrams for a single memory are distributed across multiple brain regions. Nat. Commun. 13, 1799. https://doi.org/10.1038/s41467-022-29384-4

Rusu, S.I., Bos, J.J., Marchesi, P., Lankelma, J.V., Ferreira Pica, I., Gentet, L.J., Joëls, M., Pennartz, C., 2024. Offline orbitofrontal cortex reactivation depends on recency of place-reward changes and coheres with hippocampal replay. iScience 27, 109205. https://doi.org/10.1016/j.isci.2024.109205

Tayler, K.K., Tanaka, K.Z., Reijmers, L.G., Wiltgen, B.J., 2013. Reactivation of neural ensembles during the retrieval of recent and remote memory. Curr. Biol. CB 23, 99–106. https://doi.org/10.1016/j.cub.2012.11.019

Thiffault, I., Speca, D.J., Austin, D.C., Cobb, M.M., Eum, K.S., Safina, N.P., Grote, L., Farrow, E.G., Miller, N., Soden, S., Kingsmore, S.F., Trimmer, J.S., Saunders, C.J., Sack, J.T., 2015. A novel epileptic encephalopathy mutation in KCNB1 disrupts Kv2.1 ion selectivity, expression, and localization. J. Gen. Physiol. 146, 399–410. https://doi.org/10.1085/jgp.201511444

Titley, H.K., Watkins, G.V., Lin, C., Weiss, C., McCarthy, M., Disterhoft, J.F., Hansel, C., 2020. Intrinsic Excitability Increase in Cerebellar Purkinje Cells after Delay Eye-Blink Conditioning in Mice. J. Neurosci. 40, 2038–2046. https://doi.org/10.1523/JNEUROSCI.2259-19.2019

Vierra, N.C., O'Dwyer, S.C., Matsumoto, C., Santana, L.F., Trimmer, J.S., 2021. Regulation of neuronal excitation-transcription coupling by Kv2.1-induced clustering of somatic L-type Ca2+ channels at ER-PM junctions. Proc. Natl. Acad. Sci. U. S. A. 118, e2110094118. https://doi.org/10.1073/pnas.2110094118

Weiss, C., Kronforst-Collins, M.A., Disterhoft, J.F., 1996. Activity of hippocampal pyramidal neurons during trace eyeblink conditioning. Hippocampus 6, 192–209. https://doi.org/10.1002/(SICI)1098-1063(1996)6:2<192::AID-HIPO9>3.0.CO;2-R

Wilkars, W., Liu, Z., Lewis, A.S., Stoub, T.R., Ramos, E.M., Brandt, N., Nicholson, D.A., Chetkovich, D.M., Bender, R.A., 2012. Regulation of axonal HCN1 trafficking in perforant path involves expression of specific TRIP8b isoforms. PloS One 7, e32181. https://doi.org/10.1371/journal.pone.0032181

Zhang, W., Linden, D.J., 2003. The other side of the engram: experience-driven changes in neuronal intrinsic excitability. Nat. Rev. Neurosci. 4, 885–900. https://doi.org/10.1038/nrn1248

Acknowledgments:

We thank all past and current members of the Frick and Bontempi laboratories for fruitful discussions and comments pertaining to the advancement of this project, in particular Elodie Cougouilles for assistance with behavioral experiments and Francesca Bettoni for assistance with neuronal reconstructions. We thank Aline Desmedt for making her behavioral equipment available to us. We thank the genotyping and animal housing facilities of INSERM U1215 Neurocenter Magendie for ensuring the welfare of the laboratory animals. We thank Bordeaux Imaging Center a service unit of the CNRS-INSERM and Bordeaux University, member of the national infrastructure France BioImaging supported by the French National Research Agency (ANR-10-INBS-04), particularly engineers Dr. Monica Fernandez Monreal and Sebastien Marais for their technical assistance with microscopy and image analysis.

Funding:

Agence National de la Recherche grant (AF, BB), The LabEx BRAIN funding (BB, AF), INSERM endowment (AF), State Scholarship of the China Research Council (LZ), University of the Basque Country - PIFBUR/20 (MGC)

Author contributions:

Conceptualization: SH, MG, BB, AF
Experiments: SH, LZ, MG, RDS, MGC, KLC, ON
Funding acquisition: LZ, MGC, BB, AF
Project administration: BB, AF
Writing – original draft: SH, LZ, MG, BB, AF
Writing – review & editing: SH, LZ, MG, ON, BB, AF

Diversity, equity, ethics, and inclusion:

We support inclusive, diverse, and equitable conduct of research. All experimental procedures were conducted in accordance with official European Guidelines for the Care and Use of Laboratory Animals (86/609/EEC), approved by the Bordeaux ethics committee under the aegis of the French Ministry of Research and followed the ARRIVE guidelines.

Competing interests:

The authors declare no competing interests.

Data and materials availability:

All data are available in the manuscript, the supplementary material or at the request to the corresponding authors.